Surface Band Structure of Electron Inversion Layers on Vicinal Planes of Si(100)

D. C. Tsui, M. D. Sturge, Avid Kamgar, and S. J. Allen, Jr.
Bell Laboratories, Murray Hill, New Jersey 07974
(Received 6 March 1978; revised manuscript received 3 May 1978)

We have found new minigaps in inversion layers on Si surfaces tilted at θ from (100) at $k_F = 0.85(2\pi/a)\sin\theta$, $(2\pi/a)\sin\theta$, and $1.15(2\pi/a)\sin\theta$. Our results confirm the surface band-structure model of Sham *et al.*, demonstrate that both intervalley and intravalley minigaps exist, and show that the minibands, expected for two-dimensional electron gas with a one-dimensional superlattice, have been realized in inversion layers with $\theta \lesssim 3°$.

Recently, Cole, Lakhani, and Stiles[1] observed an anomalous structure in the gate-voltage (V_g) dependence of the conductivity (σ) of n-channel MOSFET's (metal-oxide–semiconductor field-effect transistors) on Si(811). This structure was shown to be due to the presence of a minigap in the two-dimensional (2D) energy band of the inversion layer and the optical transitions across this gap have subsequently been observed.[2,3] Cole, Lakhani, and Stiles attributed the existence of this minigap to a 1D superlattice at the interface, whose origin was unknown. More recently, however, Sham, Allen, Kamgar, and Tsui[2] proposed an alternative explanation. They showed that, for inversion layers on high-index planes, such minigaps can result from the removal, by valley-valley interaction, of the valley degeneracies at crossings of the surface bands. This latter model predicts correctly the so-called "superlattice period" observed by Cole, Lakhani, and Stiles, and gives a more satisfactory account of the optical transitions across the minigap observed by Sham *et al.*

The model also predicts many other higher minigaps. To investigate these, we have fabricated n-channel MOSFET's on a number of Si surfaces vicinal to the (100) plane and measured the position of the minigap anomalies as a function of the tilt angle, θ, of the surfaces from (100). We have found that the lowest minigap occurs at the Fermi-wave vector $k_F = (2\pi/a - k_0)\sin\theta$ and have observed new minigaps at $k_F = k_0\sin\theta$, $(2\pi/a)\sin\theta$, and $(4\pi/a - k_0)\sin\theta$. Here, a is the lattice constant of Si and $k_0 = 0.85(2\pi/a)$ is the value of the wave vector at the conduction-band minima along the $\langle 100\rangle$ directions. These new gaps were not expected from the model of Ref. 1. While the gaps at $k_F = k_0\sin\theta$ and $(4\pi/a - k_0)\sin\theta$ were predicted in Ref. 2, and result from removal of valley degeneracies by valley-valley interactions, the new gap at $k_F = (2\pi/a)\sin\theta$ results from umklapp scattering of electrons from the same valley. These results give us direct information on the surface band structure of the inversion layer and show that the minibands, expected for a 2D electron gas with a 1D superlattice, have been realized in inversion layers with $\theta \lesssim 3°$. In the rest of this Letter, we first describe the band structure and then present our results and show that they confirm this model surface band structure.

On Si(100), the lowest sub-band of the inversion layer results from the two $\langle 100\rangle$ conduction-band valleys.[4] Removal of this twofold valley degeneracy has been treated by several authors.[5-7] As the surface is tilted at θ from (100), projection of the reciprocal-lattice vector, $\vec{G}_2 = (2\pi/a)(2,0,0)$, onto the surface gives a surface-reciprocal-lattice vector $\vec{Q}$ in the tilting direction with $Q = (4\pi/a)\sin\theta$. We let y and z be parallel and perpendicular to $\vec{Q}$, respectively, in the plane of the surface. In the absence of valley-valley interactions, the energy E of electrons in the lowest sub-band as a function of the wave vector k_z is a twofold-degenerate parabola centered at $k_z = 0$. On the other hand, E vs k_y, as illustrated in Fig. 1(a), consists of two parabolas centered at $k_y = \pm k_0\sin\theta$, one from each of the two $\langle 100\rangle$ valleys. Sham *et al.* have pointed out that removal of the twofold valley degeneracies at $k_y = 0, \pm Q/2, \pm 2Q/2, \ldots$ will give rise to minigaps in the surface bands and that the previously reported minigap can be attributed to that at $k_y = \pm Q/2$. It is obvious from Fig. 1(a) that these minigaps occur at $k_F = (2\pi/a - k_0)\sin\theta$, $k_0\sin\theta$, and $(4\pi/a - k_0)\sin\theta$. Here, k_F is related to n_s, the inversion-layer density, through $k_F = (\pi n_s)^{1/2}$. Moreover, the interaction of degenerate state from the same valley, differing in k_y by $\Delta k_y = Q, 2Q, \ldots$, will result in additional minigaps. Such intravalley umklapp processes with $\Delta k_y = Q$ will remove degeneracies at the points indicated by vertical bars in Fig. 1(a). The resulting minigaps occur at $k_y = \pm(2\pi/a - k_0)\sin\theta$, so that $k_F = (2\pi/a)\sin\theta$. Figure 1(b) illustrates all these minigaps and the resulting surface band structure, plotted in the periodic-zone scheme.

The samples used in this experiment were n-

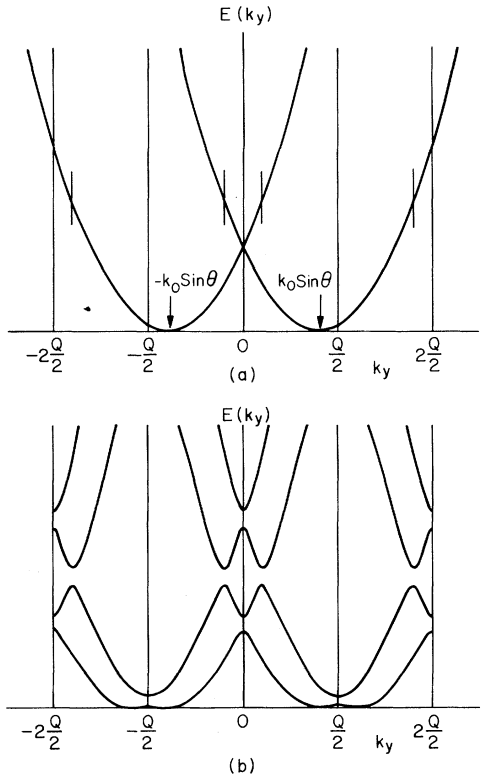

FIG. 1. E vs k_y of inversion-layer electrons on surfaces tilted at θ from (100): (a) in extended-zone scheme in the absence of valley-valley interactions and (b) in the periodic-zone scheme with degeneracies at band crossings removed. k_y is in the direction of tilt and $Q=(4\pi/a)\sin\theta$.

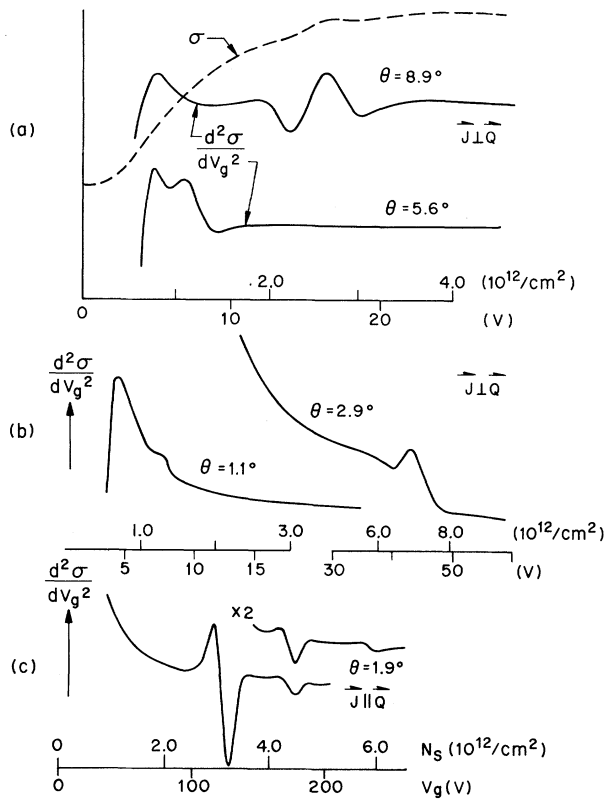

FIG. 2. σ vs V_g and $d^2\sigma/dV_g{}^2$ vs V_g at 4.2 K. (a) and (b) were taken from devices with channel perpendicular to $\vec{Q}$ and (c) from a device with channel parallel to $\vec{Q}$.

channel MOSFET's fabricated on p-type 24 Ω cm Si, which was oriented by using x rays, to better than 0.2°. Their gate oxide was thermally grown either in wet oxygen to ~1 μm thick or in dry oxygen to ~1400 Å, in both cases at 1100°C, and subsequently annealed in H_2 at 380°C. These devices have maximum channel mobility (μ) varying from ~8000 to ~20 000 cm²/V sec at 4.2 K. The electron density n_s in the channel was determined by $n_s=(C_0/e)(V_g-V_t)$, where C_0 is the capacitance of the oxide and V_t is the conduction threshold at 78 K. The minigaps were observed in dc transport and far-infrared photoresponse measurements at 4.2 K.

Figure 2 shows some data on the minigap structure in σ vs V_g and $d^2\sigma/dV_g{}^2$ vs V_g with the drain current flowing perpendicular to $\vec{Q}$. For samples with $\theta>6°$, this structure is clearly seen in σ vs V_g [Fig. 2(a)]. Cole, Lakhani, and Stiles explained this structure as a reflection, in the scattering of electrons at E_F, of the minigap structure in the density of states. They assigned its peak position as the n_s at which E_F is in the middle of the minigap, which is an increasing function of n_s. This assignment, while somewhat arbitrary, was subsequently confirmed by the spectroscopic measurements of Sham *et al.*, and we adopt it to determine n_s (and therefore k_F) at which the minigap occurs. Similar, even more pronounced, structure is also observed in the photoresponse.

The minigap structure shown in Fig. 2(a), first observed by Cole, Lakhani, and Stiles on a (811) surface ($\theta=10°$), is due to the gaps at $k_y=\pm Q/2$ in Fig. 1(b). We have observed that as θ decreases, the structure weakens and occurs at lower n_s. This observation is consistent with the fact that as θ decreases, the surface minizone decreases and the n_s required to bring E_F into the minigap decreases. Since the minigap itself decreases with decreasing n_s and with decreasing θ,[3,8] the gap structure is expected to weaken. In fact, as noted above, the structure for $\theta=5.6°$ is not strong enough to be resolved in σ vs V_g.

For the $\theta=2.9°$ and 1.1° samples, this structure

was expected at $n_s \sim 6\times10^{11}/\text{cm}^2$ and $n_s \sim 1\times10^{11}/\text{cm}^2$. However, the structure becomes so weak that it has not been seen in either $d^2\sigma/dV_g^2$ vs V_g or in the photoresponse, even though the optical tranistions across this minigap have been observed for $\theta = 2.9°$.[8] In Fig. 2(b), a new minigap structure is seen at $n_s \approx 7\times10^{12}/\text{cm}^2$ for $\theta = 2.9°$. This structure, also discernible in the 1.1° data, occurs at $k_F = k_0 \sin\theta$ and, therefore, must be due to the minigap at $k_y = 0$. The size of this gap is estimated from magnetic breakdown to be $\Delta \sim 10$ meV at $\sim 8\times10^{12}/\text{cm}^2$ for the 2.9° sample and ~3 meV at $1.7\times10^{12}/\text{cm}^2$ for $\theta = 1.1°$. Further structure in $d^2\sigma/dV_g^2$, attributable to the two higher minigaps, has been observed in 1.1° and 1.9° samples in which the current flow $\vec{J}$ is parallel to $\vec{Q}$, instead of perpendicular to it, as in the other samples. (This geometry is found to be more sensitive to minigap effects.) Data from a 1.9° sample are shown in Fig. 2(c). Besides the structure at $n_s = 3.1\times10^{12}$ cm^{-2}, which is due to the minigap at $k_F = 0.85(2\pi/a)\sin\theta$, there are two further structures, at 4.3×10^{12} and 5.4×10^{12} cm^{-2}, corresponding to $k_F = (2\pi/a)\sin\theta$ and $k_F = 1.15(2\pi/a)\sin\theta$, respectively.

Figure 3 summarizes our $\vec{J}\perp\vec{Q}$ data on the minigaps at $k_y = 0$ and $\pm Q/2$ by plotting k_F $[= (\pi n_s)^{1/2}]$, at which the minigap was observed, as a function of $\sin\theta$. The two solid lines are $k_F = 0.15(2\pi/a)\sin\theta$ and $k_F = 0.85(2\pi/a)\sin\theta$ with $a = 5.43$ Å. Deviations from the solid line seen in the data for $\theta = 5.6°$, 7.8°, and 8.9° are beyond experimental uncertainties. It should be noted that we have assumed that all the electrons populate the lowest sub-band to obtain k_F from n_s. At these low n_s, Shubnikov–de Hass measurements show that the heavy-mass sub-band is not pupulated and our assumption should be valid.[9] One possible explanation for the deviations is that the local surface orientation of the inversion layer differs by ~0.5° from the surface probed by x-ray scattering. Also, the assumption that the peak in $d^2\sigma/dV_g^2$ occurs when the Fermi level is in the center of the minigap may not be exactly valid.

It should be noted that, except for the gap at $k_0 \sin\theta$, the interactions giving rise to these minigaps involve umklapp processes and the effective potential is periodic with a periodicity of the surface lattice constant $a/2\sin\theta$. Also, since the minigap at $(2\pi/a)\sin\theta$ results from intravalley umklapp process, its existence should not be limited to multivalley semiconductors. Searches for such minigaps in hole inversion layers and in single-valley semiconductors, such as InSb,[10]

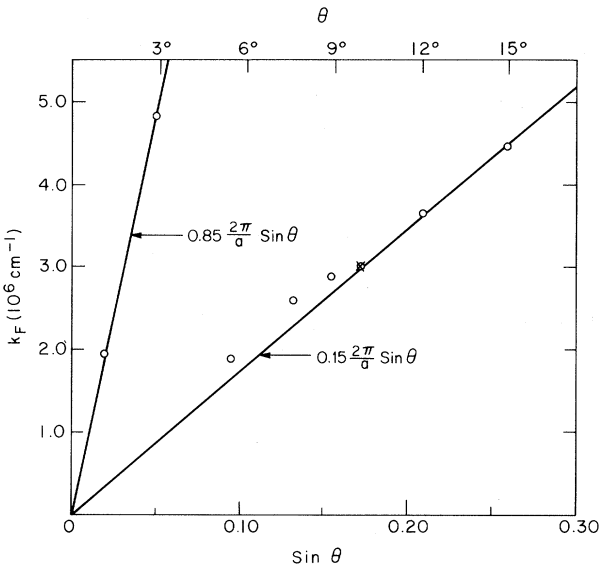

FIG. 3. A summary of $\vec{J}\perp\vec{Q}$ data on the occurrence of minigaps at $k_y = 0$ and $\pm Q/2$. $k_F = (\pi n_s)^{1/2}$, where n_s is the density at which the minigap was observed. The solid lines are $k_F = 0.15\ (2\pi/a)\sin\theta$ and $k_F = 0.85\ (2\pi/a)\sin\theta$ with $a = 5.43$ Å. The cross is from Ref. 1.

should be worthwhile.

In summary, we have found that the minigap, first reported by Cole, Lakhani, and Stiles, occurs at $k_F = (2\pi/a - k_0)\sin\theta$ and observed new minigaps at $k_F = k_0\sin\theta$, $(2\pi/a)\sin\theta$, and $(4\pi/a - k_0)\sin\theta$. These results give direct information on the surface band structure of inversion layers on tilted surfaces and show that the band structure, realized in the samples with $\theta \leq 3°$, is analogous to that expected from a 2D electron gas with a 1D superlattice. The minizones are equivalent to those resulting from a superlattice with period 141 Å for $\theta = 1.1°$ and 54 Å for $\theta = 2.9°$. The corresponding widths of the lowest bands are ~10 meV and ~50 meV, respectively. In such samples with sufficiently long electron mean free path, it should be possible to observe and to experiment with the long-anticipated electronic phenomena, such as Bloch oscillation, negative differential resistance, and Zener breakthrough, expected from such an electronic system.[11]

We acknowledge the contributions of G. Kaminsky to this work and thank J. M. Rowell and L. J. Sham for discussions.

[1]T. Cole, A. A. Lakhani, and P. J. Stiles, Phys. Rev.

Lett. 38, 722 (1977); P. J. Stiles, T. Cole, and A. A. Lakhani, J. Vac. Sci. Technol. 14, 909 (1977).

[2]L. J. Sham, S. J. Allen, A. Kamgar, and D. C. Tsui, Phys. Rev. Lett. 40, 472 (1978).

[3]D. C. Tsui and E. Gornik, Appl. Phys. Lett. 32, 365 (1978).

[4]F. Stern and W. E. Howard, Phys. Rev. 163, 816 (1967).

[5]K. Narita and E. Yamada, in *Proceedings of the Twelfth International Conference on the Physics of Semiconductors, Stuttgart, 1974*, edited by M. Pilkuhn (Teubner, Stuttgart, Germany, 1974), p. 719.

[6]F. J. Ohkawa and Y. Uemura, Surf. Sci. 58, 254 (1976).

[7]L. J. Sham and M. Nakayama, in Proceedings of the Second International Conference on Electronic Properties of 2D Systems, Berchtesgaden, 1977 (unpublished).

[8]Avid Kamgar, M. D. Sturge, and D. C. Tsui, unpublished.

[9]D. C. Tsui and G. Kaminsky, Phys. Rev. Lett. 35, 1468 (1975); W. E. Howard and F. F. Fang, Phys. Rev. B 13, 2519 (1976).

[10]A. Därr, J. P. Kotthaus, and J. F. Koch, Solid State Commun. 17, 445 (1976).

[11]L. Esaki and R. Tsu, IBM J. Res. Develop. 14, 61 (1970).

Conductivity of a Three-Component "Reactive" Percolation Model

J. W. Halley
School of Physics and Astronomy, University of Minnesota, Minneapolis, Minnesota 55455

and

W. K. Holcomb
Physics Department, University of Alabama, University, Alabama 35486

(Received 19 January 1978)

We consider a new kind of percolation model in which sites can be occupied by two kinds of "atoms," A or B, or by "molecules" formed from A and B. Introducing plausible models for conductivity we find numerically that the total sample resistivity ρ can be a nonmonotonic function of the total concentration of free and bound A. These results are qualitatively consistent with recent experiments on solid mixtures of sodium and ammonia. We discuss other features of the model qualitatively.

In recent years, there has been widespread interest in applying simple percolation models[1] to account for a variety of phenomena as diverse as disease propagation, electrical conduction in amorphous solids, and tertiary recovery of oil from porous rock.[2] We recall that a simple percolation model is specified by a lattice, and a rule for inserting conductive nodes (site percolation) or bonds (bond percolation) on the lattice. Recently Zallen[3] has introduced "polychromatic" percolation models in which the sites can be occupied by more than two kinds (colors) of entities. In the present Letter we introduce a model corresponding to three "colors" in Zallen's terminology but with an added constraint on the concentrations which arises from the condition that two of the species interact chemically to form the third. In this new model we also present the first transport calculations made for any polychromatic model. The transport results are qualitatively similar to recent experimental results[4] on the conductivity of solid mixtures of sodium and ammonia.

To describe the model, we consider two types of "atoms" A and B which can react via

$$A + B \rightleftharpoons AB \tag{1}$$

to form "molecules" AB. For a fixed ratio of the total number of A's to the total number of B's, we then have N_A free A's, N_B free B's, and N_{AB} "molecules." We let N_s be the number of lattice sites and N the total number of "atoms" (free or in molecules). We define $X_A = N_A/N_S$, $X_B = N_B/N_S$, $X_{AB} = N_{AB}/N_S$, and $X = (N_A + N_{AB})/N$. Then X_A, X_B, and X_{AB} are fixed by the following conditions. First, the lattice is filled:

$$X_A + X_{AB} + X_B = 1. \tag{2}$$

Here there is one molecule per site. Secondly, Reaction (1) is characterized by equilibrium constant K:

$$X_A X_B = K X_{AB}. \tag{3}$$

Thirdly, X is fixed by experiment. Combining